Bioresource Technology 143 (2013) 538–548

Contents lists available at SciVerse ScienceDirect

Bioresource Technology

journal homepage: www.elsevier.com/locate/biortech

Simulation and optimization of ammonia removal at low temperature for a double channel oxidation ditch based on fully coupled activated sludge model (FCASM): A full-scale study

Min Yang [a], Peide Sun [a,b,*], Ruyi Wang [a], Jingyi Han [a], Jianqiao Wang [a], Yingqi Song [a], Jing Cai [a], Xiudi Tang [a]

[a] School of Environmental Science and Engineering, Zhejiang Gongshang University, Hangzhou 310012, China
[b] Zhejiang Provincial Key Laboratory of Solid Waste Treatment and Recycling, Hangzhou 310012, China

HIGHLIGHTS

- A novel model was proposed to simulate and optimize the poor ammonia removal efficiency of a full-scale WWTP at low temperature.
- Several important kinetic parameters were determined by respirometer test.
- The optimal operating condition was DO of 3.5 mg L^{-1}, SRT of 15 d, HRT of 14 h.
- Ammonia removal efficiency would improve 19.14% under the optimal operating condition.

ARTICLE INFO

Article history:
Received 16 March 2013
Received in revised form 7 June 2013
Accepted 10 June 2013
Available online 15 June 2013

Keywords:
Full-scale
Numerical optimization
Ammonia removal
Low temperature
Fully coupled activated sludge model (FCASM)

ABSTRACT

An optimal operating condition for ammonia removal at low temperature, based on fully coupled activated sludge model (FCASM), was determined in a full-scale oxidation ditch process wastewater treatment plant (WWTP). The FCASM-based mechanisms model was calibrated and validated with the data measured on site. Several important kinetic parameters of the modified model were tested through respirometry experiment. Validated model was used to evaluate the relationship between ammonia removal and operating parameters, such as temperature (T), dissolved oxygen (DO), solid retention time (SRT) and hydraulic retention time of oxidation ditch (HRT). The simulated results showed that low temperature have a negative effect on the ammonia removal. Through orthogonal simulation tests of the last three factors and combination with the analysis of variance, the optimal operating mode acquired of DO, SRT, HRT for the WWTP at low temperature were 3.5 mg L^{-1}, 15 d and 14 h, respectively.

1. Introduction

Activated sludge process was regarded as one of the most effective and economical way in treating wastewater. Various functional microorganisms and other matter made up of the activated sludge. Nitrification bacteria and denitrification bacteria were two kinds of the functional microorganism which contributed to the nitrogen removal. In recent years, an increasing number of studies showed that temperature played an important role in nitrification and denitrification process. Ammonia oxidation was not only the main way of nitrogen removal, but also the foundation of other nitrogen removal reaction, such as nitrification, partial nitrification, and anammox (Kumar and Lin, 2010; Lan et al., 2011; Waki et al., 2010). The optimum growth temperature of majorities of the nitrifying bacteria was 30–35 °C. when temperature was below 15 °C, the activity of nitrifying bacteria reduced and as a result, the nitrification rates dropped significantly (Sudarno et al., 2011; Sun et al., 2010). However, in many places of the world temperature difference varied greatly between summer and winter. It led to that many wastewater treatment plant (WWTP) had satisfying nitrogen removal efficiency in summer, whereas very poor in winter. And so was in China. Moreover, the effluent quality of wastewater treatment was becoming more and more stringent. So it was necessary to figure out a cost-effective way to optimize the process of WWTP at different seasons.

It was well known that the biochemical reaction processes in activated sludge system were complicated, nonlinear and difficult

* Corresponding author at: School of Environmental Science and Engineering, Zhejiang Gongshang University, Hangzhou 310012, China. Tel.: +86 13336182281; fax: +86 0571 88905799.
E-mail address: pdsun@126.com (P. Sun).

0960-8524/$ - see front matter © 2013 Elsevier Ltd. All rights reserved.
http://dx.doi.org/10.1016/j.biortech.2013.06.029

Table 1
Definition of modified FCASM components.

No.	Symbol	Definition	Units
1	S_{O_2}	Dissolved oxygen	$g(O_2)\ m^{-3}$
2	S_A	Acetate	$g(COD)\ m^{-3}$
3	S_{PRO}	Propionate	$g(COD)\ m^{-3}$
4	S_F	Fermentable, readily biodegradable organic substrates	$g(COD)\ m^{-3}$
5	S_I	Soluble inert organic matters	$g(COD)\ m^{-3}$
6	S_{NH_4}	Ammonium plus ammonia nitrogen	$g(N)\ m^{-3}$
7	S_{NO_3}	Nitrate nitrogen	$g(N)\ m^{-3}$
8	S_{NO_2}	Nitrite nitrogen	$g(N)\ m^{-3}$
9	S_{NO}	Nitric oxide	$g(N)\ m^{-3}$
10	S_{N_2O}	Nitrous oxide	$g(N)\ m^{-3}$
11	S_{N_2}	Nitrogen	$g(N)\ m^{-3}$
12	S_{PO_4}	Inorganic soluble phosphorus, primarily orthophosphates	$g(P)\ m^{-3}$
13	S_{ALK}	Bicarbonate alkalinity	$mol(HCO_3^-)\ m^{-3}$
14	S_{IC}	Inorganic carbon	$g(COD)\ m^{-3}$
15	S_{H_2}	Hydrogen	$g(COD)\ m^{-3}$
16	S_{CH_4}	Methane	$g(COD)\ m^{-3}$
17	X_I	Inert particulate organic material	$g(COD)\ m^{-3}$
18	X_S	Slowly biodegradable substrates	$g(COD)\ m^{-3}$
19	X_{OH}	Aerobic heterotrophic organisms	$g(COD)\ m^{-3}$
20	$X_{STO,OH}$	A cell internal storage product of aerobic heterotrophic organisms	$g(COD)\ m^{-3}$
21	X_{DNZ}	Nitric oxide-reducing bacteria	$g(COD)\ m^{-3}$
22	$X_{STO,DNZ}$	A cell internal storage product of nitric oxide-reducing bacteria	$g(COD)\ m^{-3}$
23	X_{DNQ}	Nitrous oxide-reducing bacteria	$g(COD)\ m^{-3}$
24	$X_{STO,DNQ}$	A cell internal storage product of nitrous oxide-reducing bacteria	$g(COD)\ m^{-3}$
25	X_{DNS}	Nitrite reducing organisms	$g(COD)\ m^{-3}$
26	$X_{STO,DNS}$	A cell internal storage product of nitrite reducing organisms	$g(COD)\ m^{-3}$
27	X_{DNB}	Nitrate reducing organisms	$g(COD)\ m^{-3}$
28	$X_{STO,DNB}$	A cell internal storage product of nitrate reducing organisms	$g(COD)\ m^{-3}$
29	X_{NS}	Ammonium oxidizing autotrophs	$g(COD)\ m^{-3}$
30	X_{NB}	Nitrite oxidizing autotrophs	$g(COD)\ m^{-3}$
31	X_{ACID}	Acid-producing bacteria	$g(COD)\ m^{-3}$
32	X_{ACET}	Hydrogen production of acetic acid bacteria	$g(COD)\ m^{-3}$
33	X_{MAC}	Turn acetic acid methane-producing bacteria	$g(COD)\ m^{-3}$
34	X_{MH_2}	Turn hydrogen methane-producing bacteria	$g(COD)\ m^{-3}$
35	X_{PAO}	Non-denitrifying phosphorus-accumulating organisms	$g(COD)\ m^{-3}$
36	$X_{PP,PAO}$	Polyphosphate of non-denitrifying phosphorus-accumulating organisms	$g(P)\ m^{-3}$
37	$X_{PHA,PAO}$	A cell internal storage product of non-denitrifying phosphorus-accumulating organisms	$g(COD)\ m^{-3}$
38	$X_{GLY,PAO}$	A cell internal storage product of non-denitrifying phosphorus-accumulating organisms	$g(COD)\ m^{-3}$
39	X_{DPB}	Denitrifying phosphorus-accumulating bacteria	$g(COD)\ m^{-3}$
40	$X_{PP,DPB}$	Polyphosphate of denitrifying phosphorus-accumulating bacteria	$g(P)\ m^{-3}$
41	$X_{PHA,DPB}$	A cell internal storage product of denitrifying phosphorus-accumulating bacteria	$g(COD)\ m^{-3}$
42	$X_{GLY,DPB}$	A cell internal storage product of denitrifying phosphorus-accumulating bacteria	$g(COD)\ m^{-3}$
43	X_{GAO}	Glycogen-accumulating organisms	$g(COD)\ m^{-3}$
44	$X_{PHA,GAO}$	A cell internal storage product of glycogen-accumulating organisms	$g(COD)\ m^{-3}$
45	$X_{GLY,GAO}$	A cell internal storage product of glycogen-accumulating organisms	$g(COD)\ m^{-3}$
46	X_{TSS}	Total suspended solids	$g(TSS)\ m^{-3}$
47	X_{MeOH}	Metal hydrolyzate	$g(TSS)\ m^{-3}$
48	X_{MeP}	Chemical phosphorus	$g(TSS)\ m^{-3}$

to describe. Activated sludge models proposed in 1980s and 1990s by the International Water Association (IWA) (Gujer et al., 1999, 1995; Henze et al., 1987, 1999), were proved to be useful and powerful tools to simulate and optimize activated sludge system (Souza et al., 2008; Xie et al., 2011). Varieties software containing a number of activated sludge models were developed to simulate and optimize the biochemical reaction process, which provided an important platform for process optimization (Ferrer et al., 2008; Muschalla et al., 2009). Nevertheless, most of the models could not directly reflect the effect of temperature on biochemical reaction processes. As a result, the optimized conclusion was not convincing.

Fully coupled activated sludge model (FCASM) put forward a new concept of interaction between different microorganism communities and ambient conditions (Sun et al., 2009). Temperature was coupled into the kinetic reaction equation directly. Hence, FCASM could intuitively reflex the effect of temperature on reaction rate of biochemical processes without changing the kinetic parameters. This would be more convenient to calibrate and validate the model. Considering majority of wastewater were made up of the domestic sewage and industrial wastewater in China, the negative effect of inhibitory factors on biochemical reactions was also included in FCASM. Moreover, floras were divided into eight categories in FCASM, which described the metabolic process of microorganism more detailedly. It was already proved that FCASM could be used to instruct the operation of municipal WWTP, in which the wastewater contained about thirty percent industrial wastewater (Lou et al., 2008). In order to describe the activated sludge system more comprehensively, FCASM also should contain some physical and chemical process, anaerobic digestion process, the full process of hydrolysis. Because these processes would also affect the accuracy of the predicted results (Seco et al., 2004).

In this study, the mechanistic model was used to optimize a double channel oxidation ditch WWTP with poor ammonia removal efficiency at low temperature. Through developing and extending a mechanistic model based on FCASM, a numerical model about the double channel oxidation ditch WWTP (Shengxin WWTP) was established. The data tested in field were used to calibrate and validate the modified model. Then the validated model

Table 2
Representative kinetic equations.

No.	Process	Rate expression
Hydrolysis		
1	Aeration	$k_{HYD} e^{\theta_{HYD}(T-20)} M_{O_2} \frac{X_S/(X_{OH}+X_{DNS}+X_{DNB}+X_{PAO}+X_{DPB}+X_{GAO}+X_{ACID})}{K_X+X_S/(X_{OH}+X_{DNS}+X_{DNB}+X_{PAO}+X_{DPB}+X_{GAO}+X_{ACID})}$ $(X_{OH}+X_{DNS}+X_{DNB}+X_{PAO}+X_{DPB}+X_{GAO}+X_{ACID})$
2	Anoxic	$k_{HYD}\eta_{NOX} e^{\theta_{HYD}(T-20)} I_{O_2} M_{NO_X} \frac{X_S/(X_{OH}+X_{DNS}+X_{DNB}+X_{PAO}+X_{DPB}+X_{GAO}+X_{ACID})}{K_X+X_S/(X_{OH}+X_{DNS}+X_{DNB}+X_{PAO}+X_{DPB}+X_{GAO}+X_{ACID})}$ $(X_{OH}+X_{DNS}+X_{DNB}+X_{PAO}+X_{DPB}+X_{GAO}+X_{ACID})$
3	Anaerobic	$k_{HYD}\eta_{fe} e^{\theta_{HYD}(T-20)} I_{O_2} I_{NO_X} \frac{X_S/(X_{OH}+X_{DNS}+X_{DNB}+X_{PAO}+X_{DPB}+X_{GAO}+X_{ACID})}{K_X+X_S/(X_{OH}+X_{DNS}+X_{DNB}+X_{PAO}+X_{DPB}+X_{GAO}+X_{ACID})}$ $(X_{OH}+X_{DNS}+X_{DNB}+X_{PAO}+X_{DPB}+X_{GAO}+X_{ACID})$
X_{OH} (aerobic heterotrophic bacterial)		
4	Aerobic storage of S_A	$k_{STO} e^{\theta_{STO}(T-20)} \frac{S_{O_2}}{K_{O_2,H}+S_{O_2}} \frac{S_A}{K_{A,H}+S_A} X_{OH}$
5	Aerobic Storage of S_{Pro}	$k_{STO} e^{\theta_{STO}(T-20)} \frac{S_{O_2}}{K_{O_2,H}+S_{O_2}} \frac{S_{PRO}}{K_{PRO,H}+S_{PRO}} X_{OH}$
6	Aerobic growth	$\mu_{OH,STO} e^{\theta_{OH}(T-20)} \frac{S_{O2}}{K_{O2,H}+S_{O2}} \frac{S_{NH4}}{K_{NH4,H}+S_{NH4}} \frac{S_{ALK}}{K_{ALK,H}+S_{ALK}} \frac{S_{PO4}}{K_{PO4,H}+S_{PO4}} \frac{X_{STO,OH}/X_{OH}}{K_{STO}+X_{STO,OH}/X_{OH}} X_{OH}$
7	Aerobic growth on S_F	$\mu_{OH,S} e^{\theta_{OH}(T-20)} M_{O2} M_{NH4} M_{PO4} \frac{S_F}{K_F+S_F} \frac{S_F}{S_F+S_A+S_{PRO}} X_{OH}$
8	Aerobic growth on S_A	$\mu_{OH,S} e^{\theta_{OH}(T-20)} M_{O2} M_{NH4} M_{PO4} \frac{S_A}{K_A+S_A} \frac{S_A}{S_F+S_A+S_{PRO}} X_{OH}$
9	Aerobic growth on S_{Pro}	$\mu_{OH,S} e^{\theta_{OH}(T-20)} M_{O2} M_{NH4} M_{PO4} \frac{S_{PRO}}{K_{PRO}+S_{PRO}} \frac{S_{PRO}}{S_F+S_A+S_{PRO}} X_{OH}$
X_{ACID} (acid-producing bacteria)		
10	Ferment	$\mu_{ACID} I_{O_2} M_{NH_4} M_{PO_4} \frac{S_F}{K_F+S_F} \frac{K_A}{K_A+S_A} \frac{K_{H_2}}{K_{H_2}+S_{H_2}} X_{ACID}$
X_{ACET} (Hydrogen production of acetic acid bacteria)		
11	S_{PRO} converted to acetic acid	$\mu_{ACET} I_{O_2} M_{NH_4} M_{PO_4} \frac{S_{PRO}}{K_{PRO}+S_{PRO}} \frac{K_A}{K_A+S_A} \frac{K_{H_2}}{K_{H_2}+S_{H_2}} X_{ACET}$
X_{MAC} (turn acetic acid methane-producing bacteria) X_{MH2} (turn hydrogen methane-producing bacteria)		
12	Acetic acid convert to methane	$\mu_{MAC} I_{O_2} M_{NH_4} M_{PO_4} \frac{S_A}{K_A+S_A} X_{MAC}$
13	Hydrogen convert to methane	$\mu_{MH_2} I_{O_2} M_{NH_4} M_{PO_4} \frac{S_{H_2}}{K_{H_2}+S_{H_2}} \frac{S_{IC}}{K_C+S_{IC}} X_{MH_2}$
Oxygen transport		
14	Dissolved oxygen transfer	$K_{La_{O_2}} (S_{O_2} - S^*_{O_2})$
Collaborative precipitation of phosphorus		
15	Precipitation	$K_{PRE} S_{PO_4} X_{MEOH}$
16	Solution	$K_{PRE} X_{MEP}$

was used to optimize the process of WWTP under different operating conditions and evaluate the performance in terms of the effluent quality. Finally, an optimum operating condition of the full-scale plant was determined to treat the poor efficiency of ammonia removal at low temperature.

2. Model adjustment

The model used in this work was based on fully coupled activated sludge model (FCASM), through some extensions and improvements to describe the activated sludge system more comprehensively.

2.1. Assumptions and improvement

In general, the elementary assumptions and mechanism of the modified model in this study were the same to those of FCASM (Sun et al., 2009). Following modifications were done: (i) temperature was coupled into kinetic rate equations directly as a variable. (ii) Physical and chemical processes of the dissolved oxygen transferred, as well as phosphorus synergistic precipitation in the activated sludge system were taken into account. Whitman's "two-film theory" (Whitman, 1962) was used to describe the transfer of dissolved oxygen from gas to liquid phase. Phosphorus precipitation process could be ascribed to the hydrolysis of metal hydroxide in the wastewater. Mutually, the precipitation would be dissolved when the pH changed (Gujer et al., 1995). (iii) Easily degradable substrate (S_S) was divided into fermentation product S_F (short-chain fatty acids, VFA not included), acetate (S_A) and propionate (S_{PRO}), which could be directly and simultaneously used by heterotrophic bacteria to maintain their own growth and reproduction. (iv) Normally, the hydrolysis process of slowly biodegradable substrate (X_S) caused by heterotrophic bacteria was happened in aerobic condition. Hydrolysis process also existed in anoxic and anaerobic conditions, although the hydrolysis rate was slower than that in aerobic mode (Gujer et al., 1995). (v) There were two mechanisms for heterotrophic bacteria to utilize the carbon source for their growth: one was that heterotrophic bacteria directly utilize the extracellular organic carbon (Henze et al., 1987), and another one was that the heterotrophic bacteria first absorbed the extracellular organic carbon into the intracellular until the outside organic carbons were depleted, then the stored materials in intracellular were used as a substrate for their growth (Gujer et al., 1995). This model assumed that both mechanisms for heterotrophic bacteria to utilize the carbon source for their growth were existed in the activated sludge system. (vi) Denitrification was split into a four-step reaction process in the modified FCASM. The simplified bioprocess of denitrification as follow(Hiatt and Grady, 2008). X_{NS}, X_{NB}, X_{DNZ}, and X_{DNQ} were defined in Table 2:

$$NO_3^- \xrightarrow{X_{NS}} NO_2^- \quad (1)$$

$$NO_2^- \xrightarrow{X_{NB}} NO \quad (2)$$

$$NO \xrightarrow{X_{DNZ}} N_2O \quad (3)$$

$$N_2O \xrightarrow{X_{DNQ}} N_2 \quad (4)$$

Table 3
Analytical method of COD component.

Component	Methods
S_A, S_{PRO}	Liquid and gas chromatography
X_S, S_S	Intermittent respirometry test
S_I	Measurement of soluble$_{COD}$, then $S_I = S_S - S_{COD}$
S_F	$S_F = S_S$ – VFA
X_{DNB}, X_{DNS}	Respirometry test
$X_{H(total)}$	Respirometry test
X_{OH}	$X_{OH} = X_H - X_{DNS} - X_{DNB}$
X_I	$X_I = COD - S_S - S_I - X_S - X_H$

Table 4
Proportion of COD component.

Component	S_A	S_{PRO}	S_F	S_I	X_S	X_{OH}	X_{DNB}	X_{DNS}	X_I
Proportion (%)	10.8	6.4	15.3	21.3	34.8	6.7	1.4	2.7	0.6

2.2. Kinetic processes and parameters

In total 48 components including 16 soluble and 32 particle components were involved in the modified model. All these components were defined in Table 1.

According to the mechanism and assumptions, one hundred and twenty six bioprocesses were contained in modified FCASM. Majority of them were similar with the FCASM. Some representative kinetic processes of the modified model were shown in Table 2. All the parameters used in this model were listed in the Supplementary information (Tables 1 and 2).

3. Methods

3.1. Shengxin WWTP

Shengxin WWTP was located in Shaoxing city, east of China, where domestic sewage and industrial wastewater generated from the surrounding city areas were treated. The mixing proportion of domestic sewage and industrial wastewater was 6/4, resulting in some substance difficult to degrade. It included an equalized basin and primary clarifiers before three parallel activated sludge systems which consist of anaerobic tank and double channel oxidation ditch (Fig. 1). After primary clarifiers, wastewater was flowing into the anaerobic tank. The working volume of the anaerobic tank and double channel oxidation ditch were 6336 m^3 and 41,196 m^3, respectively. The DO concentration of oxidation ditch was 1.9 mg L^{-1}. The hydraulic retention times (HRTs) were 3 h and 12 h in the anaerobic tank and oxidation ditch, respectively. HRT of anoxic and aerobic zone in the oxidation ditch were 3 and 9 h, respectively. The solid retention time (SRT) of the full-scale double channel oxidation ditch was 20 d.

3.2. Wastewater characteristics

The average concentration of chemical oxygen demand (COD), suspend solids (SS), ammonia (NH_4^+—N), nitrate (NO_3^-—N), nitrite (NO_2^-—N) and phosphate (PO_4^{3-}—P) in influent were 368, 209, 33, 5.8, 3.2 and 3.5 mg L^{-1}, respectively. The mixed liquor suspended solids (MLSS) and sludge volume index were 3500 mg $L^{-1}$and 95 ml g^{-1}, respectively. The average inflow of Shengxin WWTP was 3500 m3 h^{-1}.

Water sample consisted of both domestic sewage and industrial wastewater was collected from Shengxin WWTP, in which printing and dyeing wastewater (PDW) was the main ingredient of the industrial wastewater. Although the PDW have been pretreated in the factory before entered the Shengxin WWTP, the B/C ratio was lower than normal domestic sewage, because PDW contained a lot of hard-to-degrade substance, such as Cibacvron Red FB, Dispersal Yellow C 4R, Solophenyl Orang T4RL. Sometimes, these substances are toxic to microorganisms then inhibit the growth of microorganisms. And also these substances were the main components of the inert materials classified in the model.

In the modified model, organic matter in the influent were fractionized to fermentable, readily biodegradable organic compounds (S_F), volatile fatty acids (VFA, including acetate (S_A) and propionate (S_{Pro}), inert soluble organic compounds (S_I), slowly biodegradable organic compounds (X_S), inert particular organic compounds (X_I) and some microorganisms. The analytical methods of the organic matter components were listed in Table 3. Results were shown in Table 4. The aggregated proportion of S_I and X_I was 21.9%, which probably resulted in the high COD concentration in the effluent.

3.3. Respirometric test

3.3.1. Respirometric set-up

A closed water-sealed respirometric set-up was used to characterize the activated sludge in off-line respirometric batch test. The

Table 5
Calibrated and determined stoichiometric and kinetic parameters used in this study (20 °C).

Parameters	Definition	Value	Units	Source[a]
Y_{ACID}	Yield coefficient for acid-producing bacteria	0.1	gCOD·gCOD^{-1}	1
Y_{ACET}	Yield coefficient for Hydrogen production of acetic acid bacteria	0.1	gCOD·gCOD^{-1}	1
Y_{MAC}	Yield coefficient for methanogens acetate	0.04	gCOD·gCOD^{-1}	1
$Y_{OH,O2}$	Yield coefficient for heterotrophic biomass	0.49	gCOD·gCOD^{-1}	2
Y_{MH2}	Yield coefficient for Hydrogen methane-producing bacteria	0.04	gCOD·gCOD^{-1}	1
μ_{ACID}	Specific growth rate of acid-producing bacteria	1.2	d^{-1}	1
μ_{ACET}	Specific growth rate of Hydrogen production of acetic acid bacteria	1.2	d^{-1}	1
μ_{MAC}	Specific growth rate of methanogens	1.4	d^{-1}	1
$K_{S,AC}$	Half-saturation constant of acid-producing bacteria on S_F	0.2	gCOD m^{-3}	1
K_{CH4}	Half-saturation constant of methane	0.16	gCOD m^{-3}	1
b_{AC}	Decay coefficient of acid-producing bacteria	0.08	d^{-1}	1
b_{MAC}	Decay coefficient of the Methanogens	0.004	d^{-1}	1
μ_{OH}	Specific growth rate of heterotrophic biomass	3	d^{-1}	2
$b_{OH,O2}$	Decay coefficient of the heterotrophic biomass	0.31	d^{-1}	2
μ_{NS}	Specific growth rate of the nitrate bacteria	0.24	d^{-1}	2
μ_{NB}	Specific growth rate of the nitrite bacteria	0.504	d^{-1}	2
b_{NS}	Decay coefficient of the nitrate bacteria	0.21	d^{-1}	2
b_{NB}	Decay coefficient of the nitrite bacteria	0.37	d^{-1}	2
$K_{NH4,NB}$	Half-saturation constant of ammonia	0.84	gN m^{-3}	2
$K_{NO2,NS}$	Half-saturation constant of nitrite	0.65	gN m^{-3}	2

[a] Source 1: calibrated results and source 2: determined in this study.

Table 6
Simulation and analysis of variance results of NH_4^+—N in effluent under different test conditions.[a].

No.	DO (mg L^{-1})	SRT (d)	HRT (h)	Effluent NH_4^+—N concentration (mg L^{-1})
1	1.9	10	18	11.25
2	1.9	15	10	14.62
3	1.9	20	14	9.65
4	2.9	10	14	12.57
5	2.9	15	18	8.73
6	2.9	20	10	12.98
7	3.5	10	10	13.68
8	3.5	15	14	7.93
9	3.5	20	18	7.58
k1	11.84	12.5	13.76	
k2	11.42	10.43	10.05	
k3	9.85	10.07	9.20	
Δk	1.99	2.43	4.57	
S^2	35.42	10.33	7.50	S^2_e 1.57
F	22.50592	6.563327	4.765893	F_a 9.00

[a] k1, k2 and k3 represents the results of the different levels of various factors and, Δk for the factors range; S^2 for the mean square of the various factors, S^2e for the experimental error of the mean square; the F value for each factor characterization factors significantly, F_a was the significant judgment scale.

device, schematized in Fig. 2, was made up of a stirred watertight closed respiration chamber (1.1 L). The respiration chamber was equipped with a dissolved oxygen probe (FiveGo, Mettler–Toledo) to monitor the fluctuate value of DO. The temperature of the device was maintained at 20 ± 0.5 °C in a constant temperature laboratory. The pH value was maintained at 7.0 ± 0.1.When the measured pH value of the mixed liquor did not in the expected range, acid (HCl, 1 M) or base (NaOH, 1 M) was added to adjust the pH value.

3.3.2. Seeding sludge

Seeding sludge for the experiment was taken from aeration tank of Shengxin WWTP. Two sequencing batch reactors (SBR), viz. SBR1 and SBR2, were used to measure different kinetic parameters. SBR1 was used to enrich autotrophic nitrifying system for measuring the decay rates of ammonia oxidation bacteria (AOB) and nitrite oxidizing bacteria (NOB) (Hao et al., 2009). SBR2 was cultured according to Liwarska-Bizukojc and Bizukojc (2012), and used to test the maximum specific growth rate, half-saturation constant for ammonium ions (K_A) for AOB and maximum specific growth rate, half-saturation constant for nitrite ions ($K_{NO_2^-}$) for NOB.

3.4. Decay experiment

The activated sludge applied to the decay experiment of AOB and NOB was sampled from SBR1. When the system ran steadily,

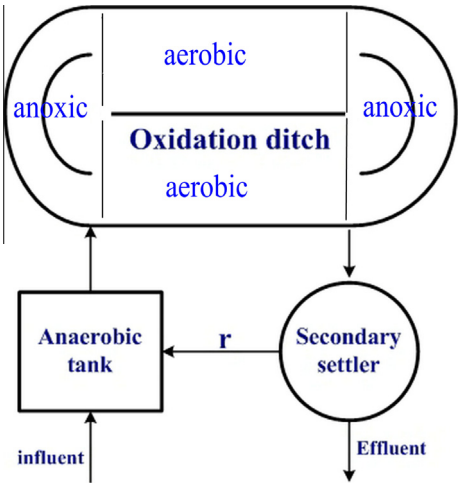

Fig. 1. Schematic of process flow of Shengxin WWTP.

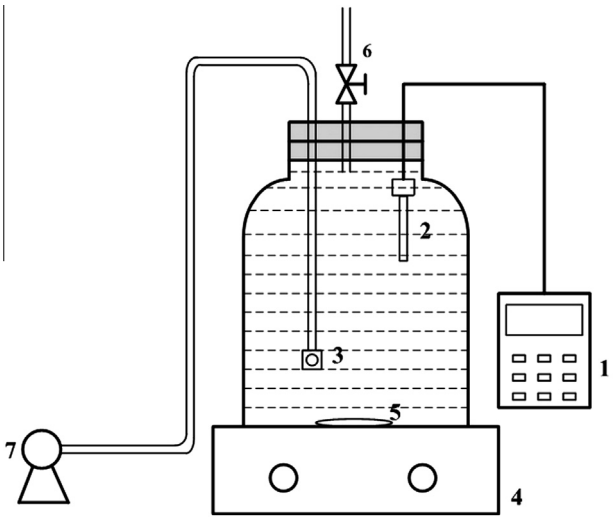

Fig. 2. The batching respirometry reactor for testing OUR: (1) DO meter, (2) DO probe, (3) aerator, (4) electromagnetic stirrer, (5) rotor, (6) vent valve,(7) air pump.

SBR1 was kept at the same environment conditions with the preset state and ready for the decay experiment. According to Hao et al. (2009), 1 L of the activated sludge took from the stable operational SBR1 was washed with the nitrobacteria lotion for three times. Then the washed sludge was shifted into the respirometric device to measuring the oxygen uptake rate (OUR) immediately. The decay rates of AOB and NOB was determined with the methods employed in previous studies (Moussa et al., 2005; Salem et al., 2006). Measuring the OUR of AOB and NOB were split in three phases. First of all, the endogenous respiration rate was measured without any substrate added. This phase lasted for 5 min. Secondly, 4 ml $NaNO_2$ was added to the respirometer chamber (resulting a 20 mg L^{-1} NO_2–N in the chamber), then the OUR of NOB was measured immediately. This phase lasted for 5 min. At last, 5 ml NH_4Cl was added (resulting a 100 mg L^{-1} NH_4–N in the chamber), and the OUR of AOB was determined. This phase lasted for 3 min. The OUR of AOB and NOB was measured once a day in following 7 days.

The decay rate of heterotrophic bacteria was measured relatively easily. 1 L returned sludge from Shengxin WWTP was washed with distilled water and added to respiration chamber. 4 ml ATU (Allylthiourea) was added into the chamber (resulting in a 20 mg L^{-1} ATU) to inhibit the growth of autotrophic bacteria.

The respirometer chamber was aerated in following 7 days and measured the OUR once a day (Vanrolleghem et al., 1999).

3.5. Specific growth rate and half-saturation constant determination

SBR2 was acclimated according to Liwarska-Bizukojc and Bizukojc (2012). After SBR2 had been performed for 15 d, the activated sludge in the system was ready for testing the kinetic parameters of nitrifying bacteria. The synthetic solution for AOB was consisted of 225 mg L^{-1} $(NH_4)_2HPO_4$, 250 mg L^{-1} $NaHCO_3$, 50 mg L^{-1} K_2HPO_4, 5 mg L^{-1} $MgSO_4{\cdot}7H_2O$ and 5 mg L^{-1} NaCl (Liwarska-Bizukojc and Bizukojc, 2012). 1 L sludge was taken from the SBR2 washed by the synthetic solution for three times. Then the washed sludge and synthetic solution (the proportion was 3/7) were introduced into the respirometer device to measure the OUR of nitrifying bacteria every 12 min among the next 18 h.

The way to measure the specific growth rate of AOB and NOB were the same except that the synthetic solutions were different. The synthetic solution for NOB was consisted of 198 mg L^{-1} $NaNO_2$ instead of $(NH_4)_2HPO_4$, while the other were the same of AOB measurement. To inhibit the growth of NOB, $NaClO_3$ was injected into the respirometer chamber, when the oxygen uptake rate of AOB was measured. Mutually, ATU was pureed into the chamber to restrain the growth of AOB when the oxygen uptake rate of NOB was tested (Liu et al., 2011).

For the purpose to measuring the specific growth rate of heterotrophic bacteria, yield coefficient of heterotrophic bacteria was determined by respirometer method at first. 1 L Sludge of aerobic tank in Shengxin WWTP washed by distilled water, with the influent of the WWTP, was introduced into the respirometer device. The OUR of heterotrophic bacteria was measured in the following 3 h when the sludge mixed with the influent immediately. Then the

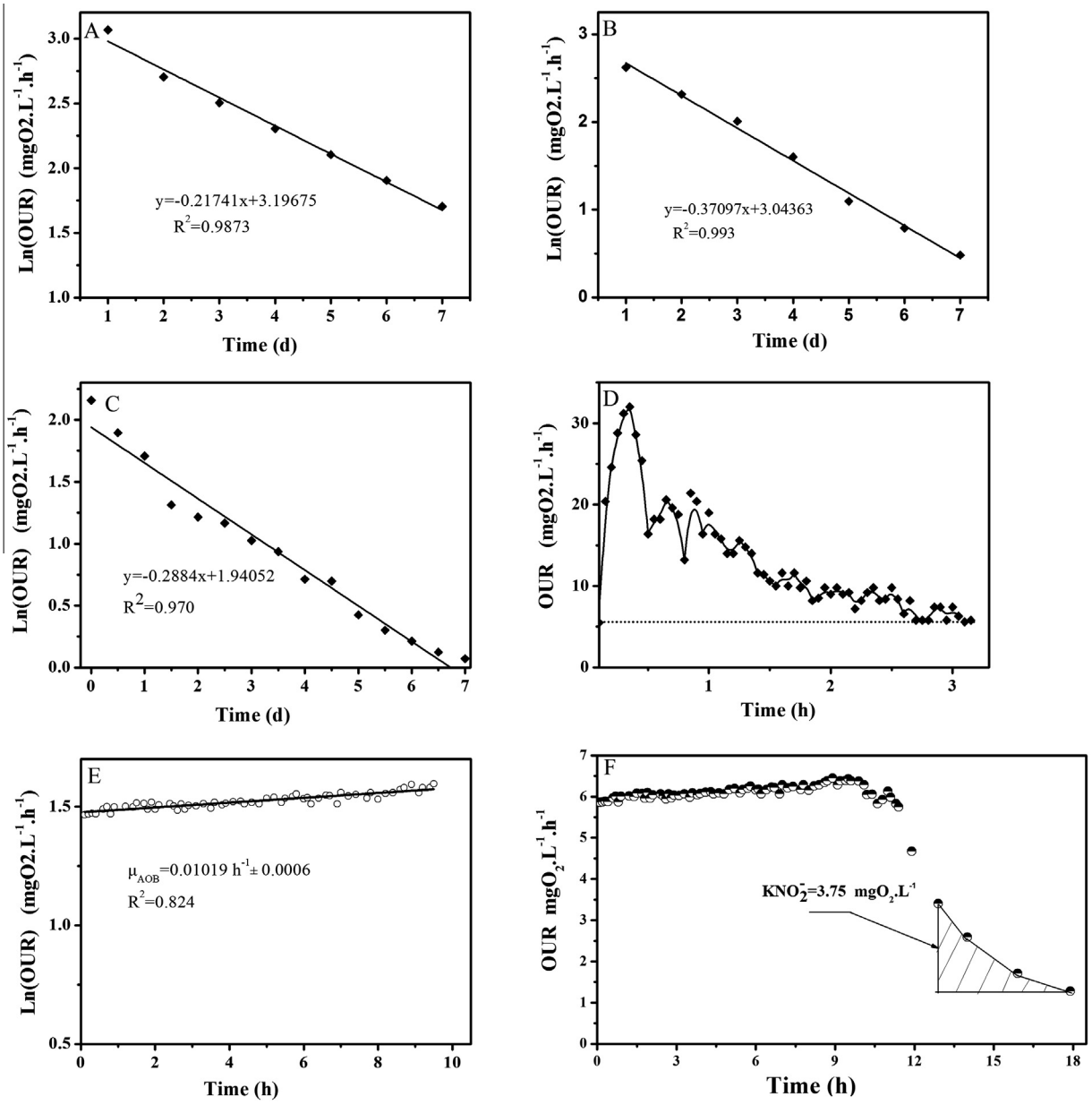

Fig. 3. Respirometric test results: decay rate of AOB (A), NOB (B) and heterotrophic bacteria (C); yield coefficient of heterotrophic bacteria (D); specific growth rate of AOB (E); half-saturation constant of NOB (F).

yield coefficient and specific growth rate of heterotrophic bacteria were measured according to Vanrolleghem et al. (1999). There were six replications of this test.

3.6. RTD studies and process modeling

The Rhodamine B was used as the tracer in this study. A 2 L aqueous solution containing 100 g Rhodamine B was prepared and then poured into anaerobic tank at the inlet. Meanwhile, the water sample was took the at the outlet of anaerobic tank, the outlet and the inlet of the oxidation ditch per 20 min. This study was continued 8 h.

The one-dimensional convection-diffusion equation combined with the biochemical reaction was used to describe the flow pattern of the process. The equation was as follow:

$$\frac{\partial C_i}{\partial t} = \frac{Q}{V}\left(\frac{1}{Pe}\frac{\partial^2 C_i}{\partial x^2} - \frac{\partial C_i}{\partial x}\right) + r(C_i) \quad (5)$$

where $r(Ci)$ refers to the biochemical reaction equation.

3.7. Analysis methods and simulation

Measurement of COD, NH_4^+—N, NO_3^-—N, NO_2^-—N, PO_4^{3-}—P, mixed liquid suspended solid (MLSS), mixed liquid volatility suspended solid (MLVSS) and sludge volume index (SVI) were performed according to the standard methods(Apha, 1998). Soluble COD was measured according to Mamais et al. (1993). The mathematical model of oxidation ditch process was simulated with MATLAB (version 7.11).

4. Results and discussion

4.1. Model calibration and validation

In order to simulate the activated sludge processes precisely, kinetic parameters should be measured and adjusted moderately. Following kinetic parameters about nitrogen removal processes were determined by the respirometric batch experiment.

4.1.1. Decay rate

The calculated decay rate of AOB and NOB were 0.2174 ± 0.0450 and 0.3710 ± 0.01237 d^{-1}, respectively (Fig. 3(A and B). These values agreed with those determined in previous researches (Moussa et al., 2005; Salem et al., 2006).

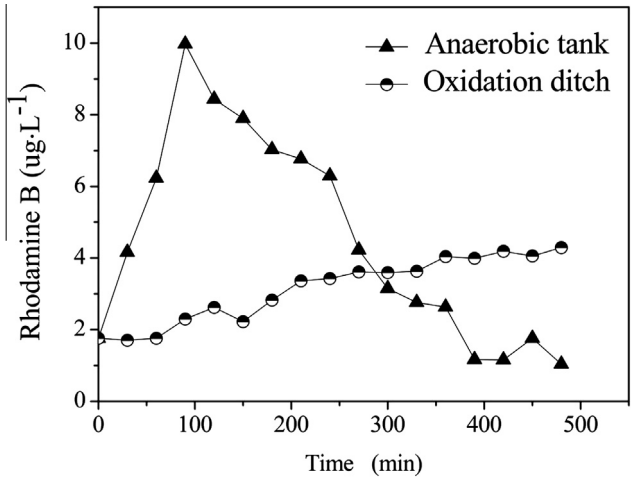

Fig. 4. Retention time distribution of tracer.

The calculated results of heterotrophic bacteria decay rate was shown in Fig. 3(C). The logarithm of the endogenous respiration rate versus time representation provides a straight line with the decay coefficient for heterotrophic biomass (lineal death), b_{OH}, as slope (Sollfrank and Gujer, 1990). The decay coefficient for heterotrophic biomass, calculated according to Ekama et al. (1986), was 0.312 ± 0.01357 d^{-1} in this study.

4.1.2. Kinetic parameters

The yield coefficient of heterotrophic biomass was measured via a respirometric batch experiment in this study. Through five parallel tests, the yield coefficient value of heterotrophic biomass was 0.492 ± 0.055625 mg cell COD (mg COD consumed)$^{-1}$ (Fig. 3D).This value was a little smaller than the typical value recommended by Gujer et al. (1995). This could be ascribed to that the influent of Shengxin WWTP was consisted of both domestic sewage and industrial wastewater. Only a few organic matters could be assimilated by heterotrophic bacteria. Moreover, some chemical matter in industrial wastewater may have a negative effect on the metabolism of heterotrophic bacteria. By measuring the yield coefficient value of heterotrophic biomass, the specific growth rate of heterotrophic bacteria was 3 d^{-1} computed according to Vanrolleghem et al. (1999). This value was not determined directly, so the deviation was inevitable existed. It needed to be adjusted in the modified model when calibrating the model.

Fig. 3(E and F) show the determined results of specific growth rate and half-saturation constant of AOB and NOB. Specific growth rate of AOB and NOB were 0.0102 ± 0.0006 and 0.021 ± 0.00467 h^{-1}. Half-saturation constant of NH_4–N for AOB and half-saturation constant of NO_2–N for NOB were 0.923 ± 0.131 $mg_{NH4}\,L^{-1}$ and 4.11 ± 0.101 $mg_{NO2}\,L^{-1}$. All of these measured values provided a powerful guarantee to ensure the simulated results more precisely.

4.1.3. RTD results and model calibration

As showed in Fig. 4, the retention time distribution of tracer in anaerobic tank and oxidation ditch was measured. The Pe coefficient was calculated with least squares methods in the MATLAB Tools. The calculated Pe coefficient values of anaerobic pool and oxidation ditch were 3.26 and 0.38, respectively. Combined one-dimensional convection-diffusion equation with the biochemical reaction, the process model was established.

In order to achieve precisely simulating results, model calibration was a necessary process. Sensitivity analysis was one of the most common and useful method for calibrating the stoichiometric and kinetic parameters of complex mathematical model (Liwarska-Bizukojc and Biernacki, 2010; Van Griensven et al., 2006). In this study, through sensitivity analysis and experiment determination, several important parameters about nitrogen removal processes were adjusted. Table 5 showed the adjustment results after sensitivity analysis and the determination results in this study. The model calibration was conducted with a set of data measured in field of Shengxin WWTP. As shown in the left side of Fig. 5, the effluent COD, NH_4^+—N, PO_4^{3-}—P concentrations during 20-day operations was measured and compared with the simulated results. It showed a good prediction tendency, indicating that the model could precisely describe the variations of the effluent COD, NH_4^+—N, PO_4^{3-}—P concentrations.

4.1.4. Model validation

Model validation was conducted with another set of data which were not used in the calibration. As shown in the right side of Fig. 5, the simulated ammonia removal, COD consumption and biological P uptake data well matched the experimental results. The average and maximum deviation between the predicted and determined COD concentrations were 7% and 18%. The simulated tendency of NH_4^+—N and PO_4^{3-}—P concentrations were also

consistent with the test values. All of these proved that the calibrated model could be used to predict the operation situation of Shengxin WWTP.

It was obvious that Shengxin WWTP was designed for the purpose of simultaneous nitrogen and phosphorus removal. However, from Fig. 4 it was clear that the phosphate removal efficiency was not satisfying. Only about 1.5 mg/L phosphate could be removed from the wastewater. There were two reasons to explain this problem. First of all, the amount of short chain fatty acids contained in the influent was too few. It was known that the short chain fatty acids (S_A and S_{PRO}) were stored into the intracellular by phosphate accumulating bacteria in the form of polyhydroxyalkanoates (PHA) at the anaerobic phase. Then PHA was used as the energy matter when phosphate accumulating bacteria absorbed the phosphorus in the aerobic segment. Nevertheless, as was shown in Table 4, aggregated proportion of S_A and S_{PRO} in this study was only 17.2%, which resulted in a lower convert ratio between organic matter and PHA, and subsequently low phosphate removal efficiency. Secondly, the wastewater was made up of domestic sewage and industrial wastewater. It contained a lot of toxic matter that may inhibit the growth and metabolism of phosphate accumulating bacteria. These factors led to the poor phosphate removal efficiency, especially the lack of short chain fatty acids resulting in that it was difficult to improve the phosphate removal efficiency through optimizing operation conditions. So in the next part of this research, the key point was to discuss how to optimize the ammonia removal at low temperature.

4.2. Model simulation of ammonia removal under different conditions

The data applied to calibrate and validate the modified model was measured in July and August. The ammonia concentration in the effluent was lower than the emission standard (5 mg L^{-1}, >12 °C; 8 mg L^{-1}, ⩽12 °C). But from November to March of the next year, the temperature was below 10 °C in most areas of China. The ammonia removal efficiency was much lower than in the summer. The average ammonia concentration in the influent of Shengxin WWTP was 50 mg L^{-1}. The average ammonia concentration in the effluent of Shengxin WWTP measured in November and March of the next year were 17 and 18 mg L^{-1}. The ammonia concentration in effluent between November and March of the next year was even much higher.

Fig. 6(A) showed the simulated effect of temperature on ammonia removal. As the temperature increased, ammonia removal rate also increased. With the increment of temperature, the activity of nitrifying bacteria became much better than that at low temperature. As a result, the nitrification rate was greatly improved. And temperature was also a key factor of denitrification. With the temperature increased, more nitrate and nitrite were converted into nitrogen. And then the total nitrogen removal efficiency was greatly improved. Therefore, in winter, it was necessary to find out optimum operating conditions for the WWTP to instead the operating conditions in usual. Furthermore, taking economic factors into account, it was unacceptable to build any new process structure in the Shengxin WWTP. So, the best solution to solve this problem was to optimize the present operating condition. For convenience, the above forty-day data were used to evaluate the effect of different operation conditions on ammonia removal by model prediction.

DO was an important impact factor on microbial reactions, almost the various processes of biological reactions were subjected to the control of the dissolved oxygen concentrations, and directly determined which process would be occurred and which process would be inhibited in the system. Fig. 6(B) illustrated the prediction results under different DO concentrations (1.9, 2.9, 3.5 mg L^{-1}). Results showed no apparent effect of different DO concentrations on COD removal. Ammonia removal rate stayed at a relatively higher and stable level under higher DO concentration than lower DO concentration. In aerobic phase, Heterotrophic bacteria and autotrophic bacteria would compete for the dissolved oxygen to maintain their growth and metabolism. The saturation content (K_S) of autotrophic bacteria for DO was higher than heterotrophic bacteria. Moreover, the existence of organic matter would also enhance the growth of heterotrophic bacteria. Nitrifiers were therefore likely to be poor competitors for oxygen at low DO concentration (Prosser, 1989).Then the nitrogen removal efficiency would be worse under low DO concentration. This was in line with the previous studies (Guo et al., 2009; Laobusnanant et al., 2009). Meanwhile, the effluent PO_4^{3-}—P concentration under lower DO value would be a little higher and have a larger fluctuation than higher DO concentration. So at low temperature, the blast volume should be increased of the full-scale plant.

Fig. 6(C) showed the simulation results with three different hydraulic retention times of the oxidation ditch. According to Xie et al. (2011), as the HRT of the aerobic tank was increased, more NH_4^+—N would be converted to NO_3^-—N and NO_2^-—N in aerobic tank, which was corresponded with the simulated results in this study. Prolonging the HRT of the oxidation ditch could increase the ammonia removal capability of the nitrifying bacteria and the phosphorous absorb capability of the phosphorous accumulating organisms. Moreover, with increased HRT, the interaction between organisms and substance would be more adequate. The COD would also distinctly decreased. As shown in Fig. 5(C), when the HRT of oxidation ditch varied from 10 to 16 h, the ammonia concentration in oxidation ditch presented an obviously decreased tendency. The effluent COD and PO_4^{3-}—P concentration also decreased with longer HRT of oxidation ditch. However, longer HRT did not necessarily result in better effluent quality and economic benefits. The longer HRT in a sense would reduce SRT, which could make the sludge loss and increase the sludge emissions, and then increase cost. Moreover, with the increment of HRT, the COD and ammonia removal efficiency would not improve but stay at a stead state. Hence, the HRT of the oxidation ditch should be balanced with other operation conditions.

The WWTP performance was also influenced by SRT and other operating conditions. Fig. 6(D) described the effect of SRT (10, 15 and 20 d) on ammonia removal by model prediction. SRT had a feeble effect on ammonia removal reflected by the figure distinctly. Also, it had a little effect on COD removal. But, as it was documented by Grady et al. (1999), changes in SRT reduced the biodegradation efficiency, and this loss of efficiency was most notable for being difficult to degrade compounds that support low biomass growth rates. Reducing SRT would reduce the biomass concentration then lead to poor effluent quality. It was widely known that longer SRT would result in a higher effluent PO_4^{3-}—P concentrations. This was chiefly because the phosphate accumulating bacteria would excessively release phosphate at the anaerobic phase. If the SRT was a little longer, more phosphate was produced, whereas PHA would not increase with the SRT increased. Then it led to poor phosphate removal efficiency. On the contrary, longer SRT would also result in higher nitrogen removal efficiency. This was mainly due to the long generation time of nitrifying bacteria and denitrifying bacteria. If SRT was too short, it would restrict the growth and reproduction of nitrifying bacteria. Therefore, a balance between different operating conditions should be found out to achieve optimal nutrient removal efficiency.

4.3. Optimum operating condition of ammonia removal

In order to solve the problem of poor ammonia removal rate at low temperature in Shengxin WWTP, an orthogonal simulation test among different DO, HRT and SRT was performed. To facilitate the

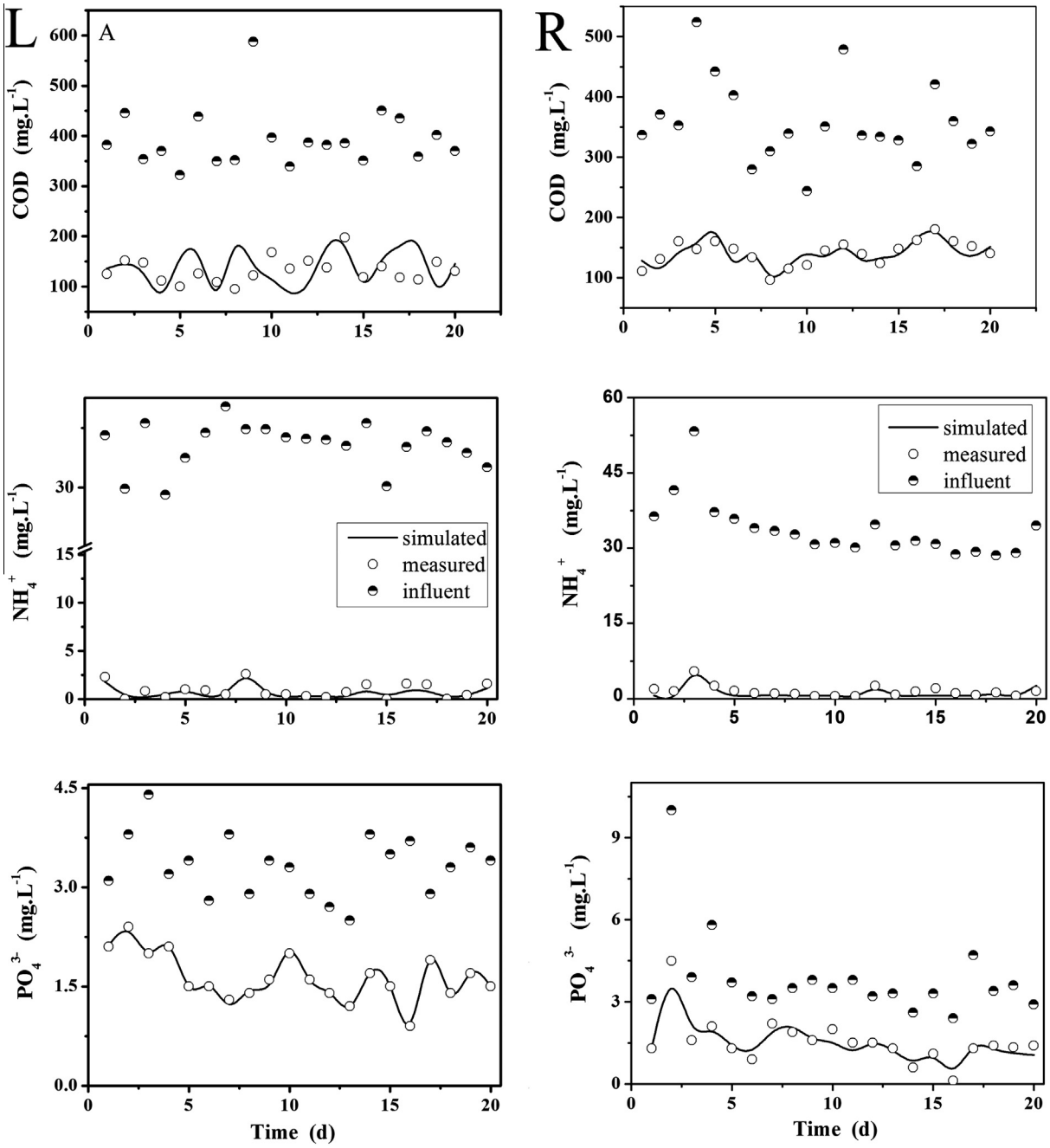

Fig. 5. Calibration (left) and validation (right) results of the modified model with the data tested in field.

simulation of the orthogonal test, the average value measured in March and November were used to evaluate the model prediction under different conditions. The measured average COD, PO_4^{3-}—P and NH_4^+—N were 380, 3.8 and 50 mg L^{-1}, respectively.

The simulation tests were performed under 10 °C. Table 6 showed the ammonia concentration under different conditions. The concentration of DO was the most significant factors that affect the removal performance. The k1 and k2 of DO were higher than k3, which meant that high dissolved oxygen was favorable to the ammonia removal at low temperature. HRT and SRT were not so significant to the ammonia removal. The k1 of HRT and SRT was a little higher than k2 and k3, which meant that short HRT and SRT were not conducive to the ammonia removal. All of these conclusions were in line with the results of single factor simulation experiment. The optimum group for ammonia removal was the HRT of 18 h, SRT of 20 d and DO of 3.5 mg L^{-1}. However, considering operation cost and removal rates of COD and PO_4^{3-}—P, the best condition for Shengxin WWTP at low temperature was then HRT of 14 h, SRT of 15 d and DO of 3.5 mg L^{-1}. Under such an operating condition, the simulated results showed that the ammonia removal efficiency would improve 19.14%. At the same time, the effluent quality would have an obvious improvement than before.

5. Conclusions

A modified model based on FCASM was used to solve the problem of poor ammonia removal rate at low temperature in a full-scale WWTP. The model after calibration and validation with a set of data measured in field was used to simulate the process.

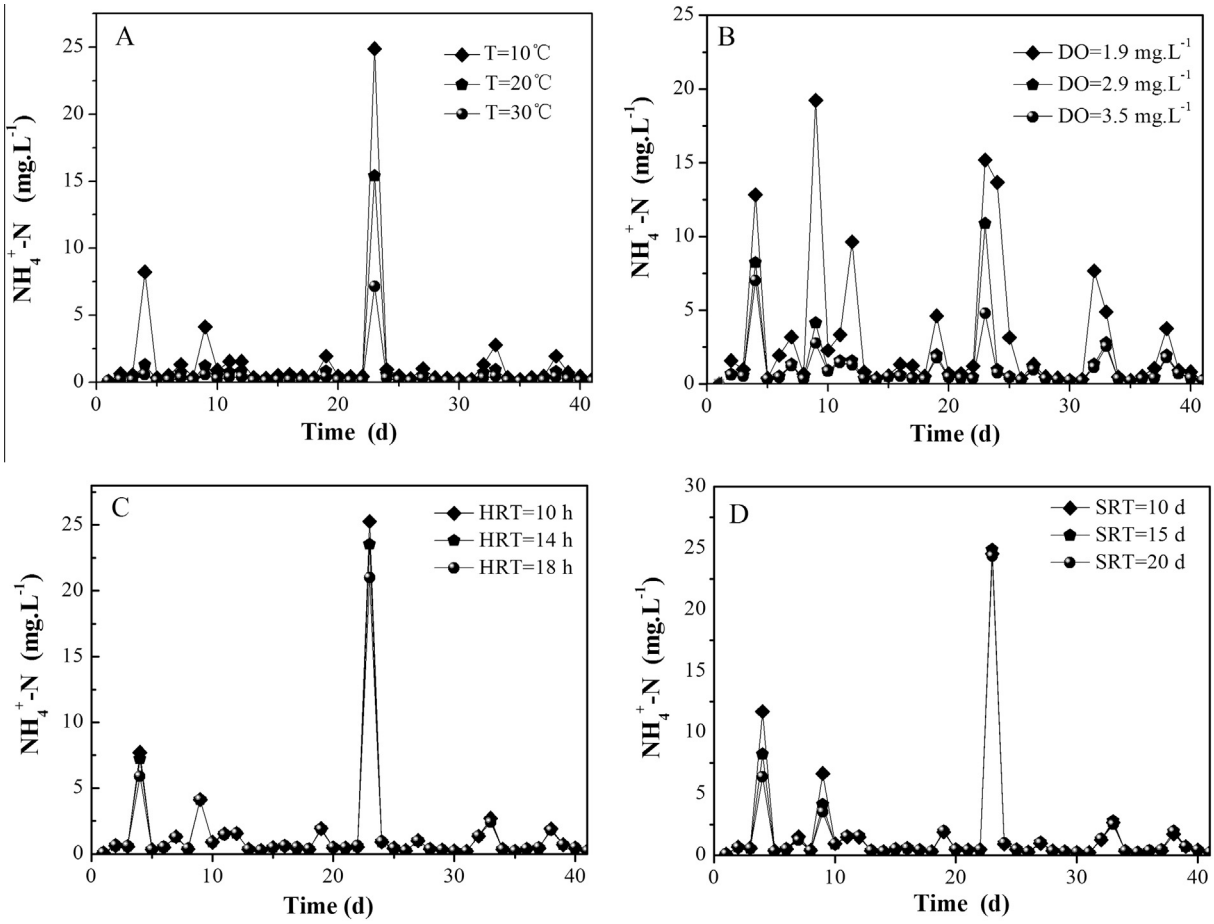

Fig. 6. Operating parameters: temperature (A), DO (B), HRT (C) and SRT (D) on the effect of ammonia removal.

Effect of operating parameters, including DO, SRT and HRT of oxidation ditch, on ammonia removal rate were evaluated. The orthogonal simulation tests showed that in order to achieve a better ammonia removal efficiency at low temperature, DO and HRT of oxidation ditch should be increased, while SRT should be decreased, compared with the previous operating conditions.

Acknowledgements

This work was financially supported by the National Natural Science Foundation of China (No. 21276236), the National "Eleventh Five-Year" Water Pollution Control and Management Technology Major Projects of China (No. 2009ZX07106-002), the Major Scientific and Technological Special Emphasis on Social Development Project of Zhejiang Province, China (Nos. 2010C03003 and 2011C13014), Scientific Research Project of Education Department of Zhejiang Province (Y201017078) and the Natural Science Foundation of Zhejiang Province, China (No. Y12E080076).

Appendix A. Supplementary data

Supplementary data associated with this article can be found, in the online version, at http://dx.doi.org/10.1016/j.biortech.2013.06.029.

References

APHA, 1998. Standard Methods for the Examination of Water and Wastewater, twentieth ed. American Public Health Association, American Water Works Association, Water Pollution Control Federation, Washington, DC.

Ekama, G.A., Dold, P.L., Marais, G.v.R., 1986. Procedures for determining influent COD fractions and the maximum specific growth rate of heterotrophs in activated sludge systems. Water Sci. Technol. 18, 91–114.

Ferrer, J., Seco, A., Serralta, J., Ribes, J., Manga, J., Asensi, E., Morenilla, J.J., Llavador, F., 2008. DESASS: a software tool for designing, simulating and optimising WWTPs. Environ. Modell Softw. 23, 19–26.

Grady Jr, C.P.L., Daigger, G.T., Lim, H.C., 1999. Biological Waste Water Treatment. Marcel Dekker, New York.

Gujer, W., Henze, M., Mino, T., Loosdrecht, M.v., 1999. Activated sludge model no. 3. Water Sci. Technol. 39, 183–193.

Gujer, W., Henze, M., Mino, T., Matsuo, T., Wentzel, M., Marais, G., 1995. The activated sludge model No. 2: biological phosphorus removal. Water Sci. Technol. 31, 1–11.

Guo, J., Peng, Y., Wang, S., Zheng, Y., Huang, H., Wang, Z., 2009. Long-term effect of dissolved oxygen on partial nitrification performance and microbial community structure. Bioresour. Technol. 100, 2796–2802.

Hao, X., Wang, Q., Zhang, X., Cao, Y., van Mark Loosdrecht, C.M., 2009. Experimental evaluation of decrease in bacterial activity due to cell death and activity decay in activated sludge. Water Res. 43, 3604–3612.

Henze, M., Grady, C., Gujer, W., Marais, G., Matsuo, T., 1987. Activated Sludge Model No. 1: IAWPRC Scientific and Technical Report No. 1. IAWPRC, London.

Henze, M., Gujer, W., Mino, T., Matsuo, T., Wentzel, M.C., Van Loosdrecht, M., 1999. Activated sludge model No. 2d, ASM2d. Water Sci. Technol. 39, 165–182.

Hiatt, W.C., Grady, C.P.L., 2008. An updated process model for carbon oxidation, nitrification, and denitrification. Water Environ. Res. 80, 2145–2156.

Kumar, M., Lin, J.G., 2010. Co-existence of anammox and denitrification for simultaneous nitrogen and carbon removal – strategies and issues. J. Hazard. Mater. 178, 1–9.

Lan, C.J., Kumar, M., Wang, C.C., Lin, J.G., 2011. Development of simultaneous partial nitrification, anammox and denitrification (SNAD) process in a sequential batch reactor. Bioresour. Technol. 102, 5514–5519.

Laobusnanant, P., Lee, S.H., Anceno, A.J., Ghosh, G.C., Kim, D.J., Pathak, B.K., Shipin, O.V., 2009. N-removal performance and underlying bacterial taxa of upflow filter bioreactor system under different dissolved oxygen and internal recycle conditions. Bioprocess Biosyst. Eng. 32, 809–818.

Liu, Y., Shi, H., Li, W., Hou, Y., He, M., 2011. Inhibition of chemical dose in biological phosphorus and nitrogen removal in simultaneous chemical precipitation for phosphorus removal. Bioresour. Technol. 102, 4008–4012.

Liwarska-Bizukojc, E., Biernacki, R., 2010. Identification of the most sensitive parameters in the activated sludge model implemented in BioWin software. Bioresour. Technol. 101, 7278–7285.
Liwarska-Bizukojc, E., Bizukojc, M., 2012. A new approach to determine the kinetic parameters for nitrifying microorganisms in the activated sludge systems. Bioresour. Technol. 109, 21–25.
Lou, J., Sun, P., Wang, R., 2008. Fully coupled activated sludge model (FCASM3) Part 3: numerical simulation of AAO process for optimum operating conditions. Acta Sci. Circumst. 2008, 2430–2437 (In Chinese).
Mamais, D., Jenkins, D., Prrr, P., 1993. A rapid physical–chemical method for the determination of readily biodegradable soluble COD in municipal wastewater. Water Res. 27, 195–197.
Moussa, M.S., Hooijmans, C.M., Lubberding, H.J., Gijzen, H.J., van Loosdrecht, M.C., 2005. Modelling nitrification, heterotrophic growth and predation in activated sludge. Water Res. 39, 5080–5098.
Muschalla, D., Schutze, M., Schroeder, K., Bach, M., Blumensaat, F., Gruber, G., Klepiszewski, K., Pabst, M., Pressl, A., Schindler, N., Solvi, A.M., Wiese, J., 2009. The HSG procedure for modelling integrated urban wastewater systems. Water Sci. Technol. 60, 2065–2075.
Prosser, I., 1989. Autotrophic nitrification in bacteria. Adv. Microb. Physiol. 30, 125–181.
Salem, S., Moussa, M.S., van Loosdrecht, M.C., 2006. Determination of the decay rate of nitrifying bacteria. Biotechnol. Bioeng. 94, 252–262.
Seco, A., Ribes, J., Serralta, J., Ferrer, J., 2004. Biological nutrient removal model No.1. Water Sci. Technol. 50, 69–78.
Sollfrank, U., Gujer, W., 1990. Characterisation of domestic wastewater for mathematical modelling of the activated sludge process. Water Sci. Technol. 23, 1057–1066.
Souza, S.M., Araujo, O.Q., Coelho, M.A., 2008. Model-based optimization of a sequencing batch reactor for biological nitrogen removal. Bioresour. Technol. 99, 3213–3223.
Sudarno, U., Winter, J., Gallert, C., 2011. Effect of varying salinity, temperature, ammonia and nitrous acid concentrations on nitrification of saline wastewater in fixed-bed reactors. Bioresour. Technol. 102, 5665–5673.
Sun, H., Yang, Q., Peng, Y., Shi, X., Wang, S., Zhang, S., 2010. Advanced landfill leachate treatment using a two-stage UASB–SBR system at low temperature. J. Environ. Sci. 22, 481–485.
Sun, P., Wang, R., Fang, Z., 2009. Fully coupled activated sludge model (FCASM): model development. Bioresour. Technol. 100, 4632–4641.
van Griensven, A., Meixner, T., Grunwald, S., Bishop, T., Diluzio, M., Srinivasan, R., 2006. A global sensitivity analysis tool for the parameters of multi-variable catchment models. J. Hydrol. 324, 10–23.
Vanrolleghem, P.A., Spanjers, H., Petersen, B., Ginestet, P., Takacs, I., 1999. Estimating (combinations of) activated sludge model No. 1 parameters and components by respirometry. Water Sci. Technol. 39, 195–214.
Waki, M., Yasuda, T., Suzuki, K., Sakai, T., Suzuki, N., Suzuki, R., Matsuba, K., Yokoyama, H., Ogino, A., Tanaka, Y., Ueda, S., Takeuchi, M., Yamagishi, T., Suwa, Y., 2010. Rate determination and distribution of anammox activity in activated sludge treating swine wastewater. Bioresour. Technol. 101, 2685–2690.
Whitman, W.G., 1962. The two film theory of gas absorption. Int. J. Heat Mass Transfer 5, 429–433.
Xie, W.M., Zhang, R., Li, W.W., Ni, B.J., Fang, F., Sheng, G.P., Yu, H.Q., Song, J., Le, D.Z., Bi, X.J., Liu, C.Q., Yang, M., 2011. Simulation and optimization of a full-scale Carrousel oxidation ditch plant for municipal wastewater treatment. Biochem. Eng. J. 56, 9–16.